Nature of yrast excitations near $N = 40$: Level structure of ^{67}Ni

S. Zhu,[1] R. V. F. Janssens,[1] M. P. Carpenter,[1] C. J. Chiara,[1,2] R. Broda,[3] B. Fornal,[3] N. Hoteling,[1,2] W. Królas,[3] T. Lauritsen,[1] T. Pawłat,[3] D. Seweryniak,[1] I. Stefanescu,[1,2] J. R. Stone,[2,4] W. B. Walters,[2] X. Wang,[1,5,*] and J. Wrzesiński[3]

[1]*Physics Division, Argonne National Laboratory, Argonne, Illinois 60439, USA*
[2]*Department of Chemistry and Biochemistry, University of Maryland, College Park, Maryland 20742, USA*
[3]*Institute of Nuclear Physics, Polish Academy of Sciences, PL-31342 Krakow, Poland*
[4]*Department of Physics, University of Oxford, OX1 3PU Oxford, United Kingdom*
[5]*Physics Department, University of Notre Dame, Notre Dame, Indiana 46556, USA*

Excited states in ^{67}Ni were populated in deep-inelastic reactions of a ^{64}Ni beam at 430 MeV on a thick ^{238}U target. A level scheme built on the previously known 13-μs isomer has been delineated up to an excitation energy of 5.3 MeV and a tentative spin and parity of $(21/2^-)$. Shell model calculations have been carried out using two effective interactions in the $f_{5/2}pg_{9/2}$ model space with a ^{56}Ni core. Satisfactory agreement between experiment and theory is achieved for the measured transition energies and branching ratios. The calculations indicate that the yrast states are associated with rather complex configurations, herewith demonstrating the relative weakness of the $N = 40$ subshell gap and the importance of multi-particle-hole excitations involving the $g_{9/2}$ neutron orbital.

I. INTRODUCTION

The presence of shell gaps with magic numbers of nucleons is a cornerstone of nuclear structure. Over the past decade it has increasingly become clear that magic numbers are not immutable but depend on the ratio of protons and neutrons [1,2]. In discussions of magic numbers, neutron number $N = 40$ has historically been a subject of debate, especially in the case of the Ni isotopes. Proton number $Z = 28$ is magic, and, for neutrons, a sizable energy gap at $N = 40$ is thought to separate the pf shell from the intruder $g_{9/2}$ state, potentially making $Z = 28$, $N = 40$ ^{68}Ni a doubly magic nucleus. Experimentally, the occurrence of shell closures in ^{68}Ni was first suggested based on the observation of a 1770-keV 0_2^+ level as the lowest excited state, followed by a 2_1^+ state of relatively high excitation energy (2034 keV) [3,4]. The discovery of several isomeric states in ^{68}Ni and in neighboring nuclei [5,6] supported the case for its magic character further, as did the results from Coulomb excitation measurements indicating a $B(E2, 2_1^+ \rightarrow 0^+)$ reduced transition probability roughly three times smaller than the corresponding value for $^{56}_{28}$Ni$_{28}$ [7,8]. However, based on recent high-precision mass measurements in the neutron-rich Ni isotopes (up to ^{73}Ni), the $N = 40$ shell closure appears to be more doubtful when inferred from changes in the two-neutron separation energies [9,10]. It has been argued in the literature that the apparent contradiction between the $B(E2)$ value and the separation energy is a consequence of the parity change across the $N = 40$ gap, with a sizable fraction of the low-lying $B(E2)$ strength residing in excited states around 4 MeV, and the 2_1^+ level being associated predominantly with a neutron-pair excitation [7,11]. The size of the $N = 40$ gap is then of the order of 2 MeV only and the corresponding discontinuity in the sequence of orbitals corresponds at most to a subshell closure.

β-decay studies [12–15] and in-beam investigations at intermediate beam energies [16–19] provide evidence for the onset of collectivity and strong polarization of the ^{68}Ni core in neighboring nuclei of the region. For example, the 2_1^+ levels in $N = 40$ ^{64}Cr [17] and ^{66}Fe [12] are located at excitation energies as low as 420 and 573 keV, respectively. More generally, the available low-spin level structures in these nuclei suggest sizable admixture of spherical and deformed components in the configurations near their ground states. These observations, combined with the large $B(E2, 2_1^+ \rightarrow 0^+)$ value measured for ^{70}Ni$_{42}$ [20], lead to the conclusion that any "island" of nuclei with indications of a significant $N = 40$ gap is rather localized. A main contributor to this situation is the monopole tensor force [21,22] between protons in the pf shell and $g_{9/2}$ neutrons, where the occupation of the latter orbital leads to the onset of deformation, as evidenced, for example, by the presence of rotational bands in neutron-rich $^{55-57}$Cr and $^{59-61}$Fe nuclei [23–27]. On the other hand, couplings of protons and/or neutrons to the ^{68}Ni core do not always result in a large polarization of the core. For example, the first excited state above the $(19/2^-)$ isomer in ^{71}Cu is located 2020 keV higher in energy, herewith mirroring the location of the 2_1^+ level in ^{68}Ni [28].

From the considerations above, it is clear that a satisfactory description of nuclear structure in this mass region is still lacking. This is also reflected in ongoing theoretical efforts to determine the most appropriate interactions for use in the calculations. In this context, the present data on the neutron-hole nucleus ^{67}Ni provide an opportunity to test the most modern interactions while investigating the nature of yrast excitations up to moderate spin.

At present, only limited information is available on the low-lying structure of ^{67}Ni. Using deep-inelastic reactions of a ^{64}Ni beam at 350 MeV on a thick ^{208}Pb target, Pawłat *et al.* [29] identified a 1008-keV isomeric state with a half-life of $T_{1/2} > 0.3$ μs decaying through coincident 314- and 694-keV transitions toward the ^{67}Ni ground state. The presence of the isomer was later confirmed in a fragmentation measurement

*Present address: Department of Physics, Florida State University, Tallahassee, Florida 32306, USA.

where a 13.3(2)-μs half-life was determined [5]. Feeding of the isomer in ^{67}Co β decay was subsequently reported [30]. These three studies [5,29,30] proposed spin and parity quantum numbers of $9/2^+$ for the long-lived state and associated this level with the occupation of the $g_{9/2}$ orbital by a single neutron. With the Nuclear Magnetic Resonance on Oriented Nuclei technique, the magnetic dipole moment of the $1/2^-$ ground state was measured to be $+0.601(5)\,\mu_N$, a value differing only slightly from the $\nu p_{1/2}$ single-particle value, a fact regarded as evidence for the strength of the $N = 40$ shell closure [31]. For the isomer, a quenched g-factor value of $|g| = 0.125(6)$ was reported in Ref. [32] and was interpreted as evidence for a 2% admixture of a $\pi(f_{7/2}^{-1}f_{5/2})_{1+}\nu g_{9/2}$ configuration involving a proton excitation across the $Z = 28$ gap into the supposedly pure $\nu g_{9/2}$ state.

Prior to the present work, no transitions feeding the isomeric state had been reported. In this work, despite the long half-life, eight states have been placed above the isomer from an investigation of prompt-delayed coincidence events in a deep-inelastic reaction with a pulsed beam.

II. EXPERIMENT

A number of experiments have demonstrated that the yrast states of hard-to-reach neutron-rich nuclei can be populated in deep-inelastic processes at beam energies 15–25% above the Coulomb barrier [33–35], allowing experimental access to high-spin structures in regions inaccessible with conventional heavy-ion-induced fusion-evaporation reactions.

The experiment was carried out with a ^{64}Ni beam delivered by the ATLAS superconducting linear accelerator at Argonne National Laboratory. The 430-MeV beam energy was chosen to correspond roughly to an energy of 20% above the Coulomb barrier in the middle of a 55 mg/cm^2 thick ^{238}U target. The beam was pulsed with a 412-ns repetition rate, each beam pulse being $\sim$0.3 ns wide. Gammasphere [36], with 100 Compton-suppressed high-purity germanium (HPGe) detectors, was used to collect events with three or more γ rays in coincidence. The data were sorted into two-dimensional (E_γ-E_γ matrices) and three-dimensional (E_γ-E_γ-E_γ cubes) histograms under various timing conditions. The prompt $\gamma\gamma\gamma$ cube (PPP cube) was incremented for γ rays observed within $\pm$20 ns of the beam burst while, in the delayed $\gamma\gamma\gamma$ cube (DDD cube), the transitions were required to occur in an interval of $\sim$40 to $\sim$800 ns after the prompt time peak (excluding the subsequent beam pulse), but within $\pm$20 ns of each other. In this way, events associated with isomeric de-excitations could be isolated and identified. The prompt-delayed-delayed (PDD) and prompt-prompt-delayed (PPD) cubes were incremented by combining prompt and delayed events. These proved critical in identifying prompt γ rays feeding isomeric levels as they revealed themselves in double-gated spectra on the known transitions below the isomer in the PDD cubes. The relations between these prompt γ rays were subsequently established by examining proper double-coincidence gates in the PPD and PPP cubes. Examples and further details of this technique can be found in Refs. [27,28].

The spins and parities of the levels were deduced from an angular-correlation analysis. In addition, considerations based

on the fact that the reactions feed yrast states preferentially, and/or on comparisons with shell-model calculations, were also taken into account. The projectile-like products of deep-inelastic reactions are usually characterized by no, or very little, alignment. Therefore, the analysis of $\gamma\gamma$ angular correlations for selected pairs of transitions is required [34,37]. In practice, in order to avoid ambiguities as much as possible in the spin assignments, at least one known stretched transition was included in the analysis.

III. RESULTS

In previous studies [5,29,30], the 314- and 694-keV transitions de-exciting the 13.3(2)-μs isomer in ^{67}Ni were assigned to the $9/2^+ \rightarrow 5/2^- \rightarrow 1/2^-$ cascade and no transition above this long-lived state was reported. As stated above, transitions feeding the isomer were initially identified in the present work by using the PDD coincidence data. A coincidence spectrum from this PDD cube with double gates placed on the 314- and 694-keV transitions is presented in Fig. 1. Besides a 1345-keV line belonging to the $2^+ \rightarrow 0^+$ transition in ^{64}Ni, three γ rays are clearly visible at 1210, 1655, and 1667 keV. The 1345-keV line originates from Coulomb excitation of the ^{64}Ni beam and is attributed to random coincidences. By double gating the PDD cube with one of the newly discovered prompt γ rays and one of the delayed transitions, their mutual coincidence relationships can be verified further. The results, displayed in Fig. 2, establish the feeding of the ^{67}Ni isomer by the 1210- and 1655-keV transitions. Finally, additional evidence was provided by the analysis of the PPD cube, where a double gate on the prompt 1655- and 1667-keV γ rays yields a delayed spectrum in which the 314- and 694-keV lines appear, consistent with the expected coincidence relationships for γ rays across the isomer. This observation also implies that the 1655- and 1667-keV transitions are in mutual, prompt coincidence.

Levels above the ^{67}Ni isomer were investigated further in the PPP cube with the 1210-, 1655-, and 1667-keV transitions as a starting point. A double gate on the latter two γ rays reveals the presence of three additional lines at 63, 172, and 708 keV (see Fig. 3). The 1655- and 1210-keV transitions are not in mutual coincidence, herewith establishing the presence of parallel decay sequences. By exploiting additional coincidence relationships, such as those displayed in Fig. 4, it was possible
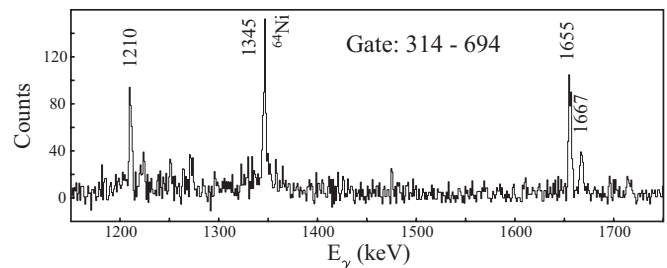

FIG. 1. Partial spectrum with double coincidence gates set on the 314- and 694-keV cascade below the ^{67}Ni $9/2^+$ isomer in the PDD cube. The spectrum shows three strong transitions feeding the $9/2^+$ state; the 1345-keV γ ray of ^{64}Ni is due to random coincidences (see text for details).
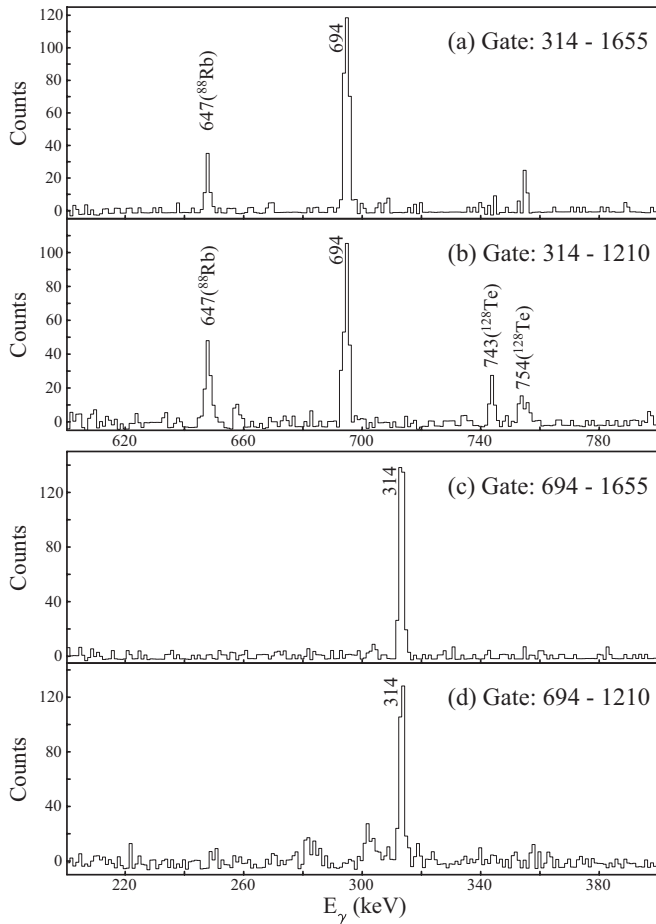
FIG. 2. Partial coincidence spectra with different gates in the PDD cube establishing the feeding of the $9/2^+$ isomeric state; see text for details. Note the change in energy scales between panels [(a), (b)] and [(c), (d)].

to propose the level scheme of Fig. 5. Thus, states at 2218, 2663, 3530, 3913, 4330, and 4502 keV were firmly established through the various competing decay paths. The ordering of the highest levels at 4565 and 5273 keV is based on the measured
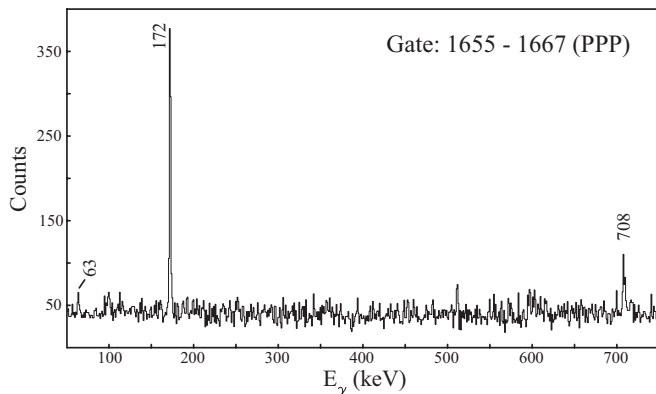

FIG. 3. Partial coincidence spectrum with double gates set on the 1655- and 1667-keV lines in the PPP cube showing the transitions from the states with highest excitation energy observed in the present work.
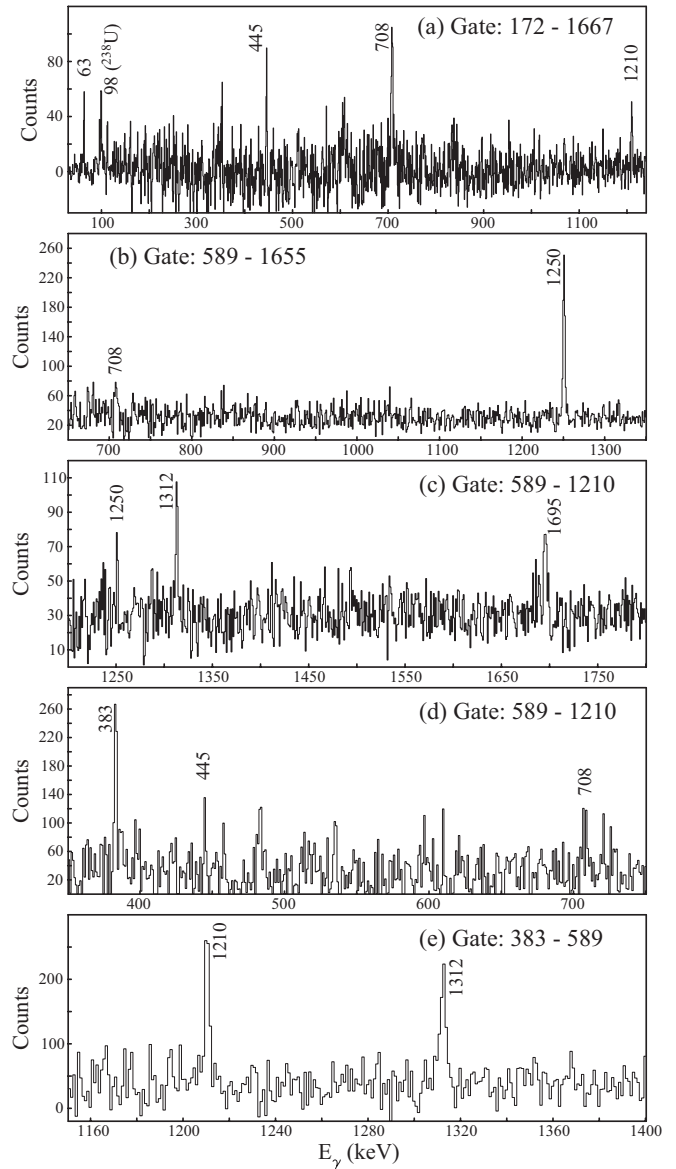

FIG. 4. Partial spectra with different gates in the PPP cube demonstrating various coincidence relationships used to establish the level scheme of Fig. 5.

γ-ray intensities. The presence of a low-energy transition of 63 keV might suggest a longer half-life for the 4565-keV state. Unfortunately, at this energy, the timing signal of the large-volume germanium detectors is rather poor. This fact, combined with the rather small intensity, made it impossible to obtain firm information on the level lifetime. However, time spectra gated on the transitions below the 4502-keV state do not provide evidence for a measurable lifetime and an upper limit of $\sim$15 ns can be given for the 4565-keV level.

Angular correlations were used to determine the multipolarity of some of the newly identified transitions. Because the yield of the 314- and 694-keV isomeric cascade was sufficient, the relevant coincidence intensities were grouped into 12 different angles θ. The measured angular-correlation pattern for this pair strongly favors a sequence with two stretched quadrupole transitions, as can be seen from the
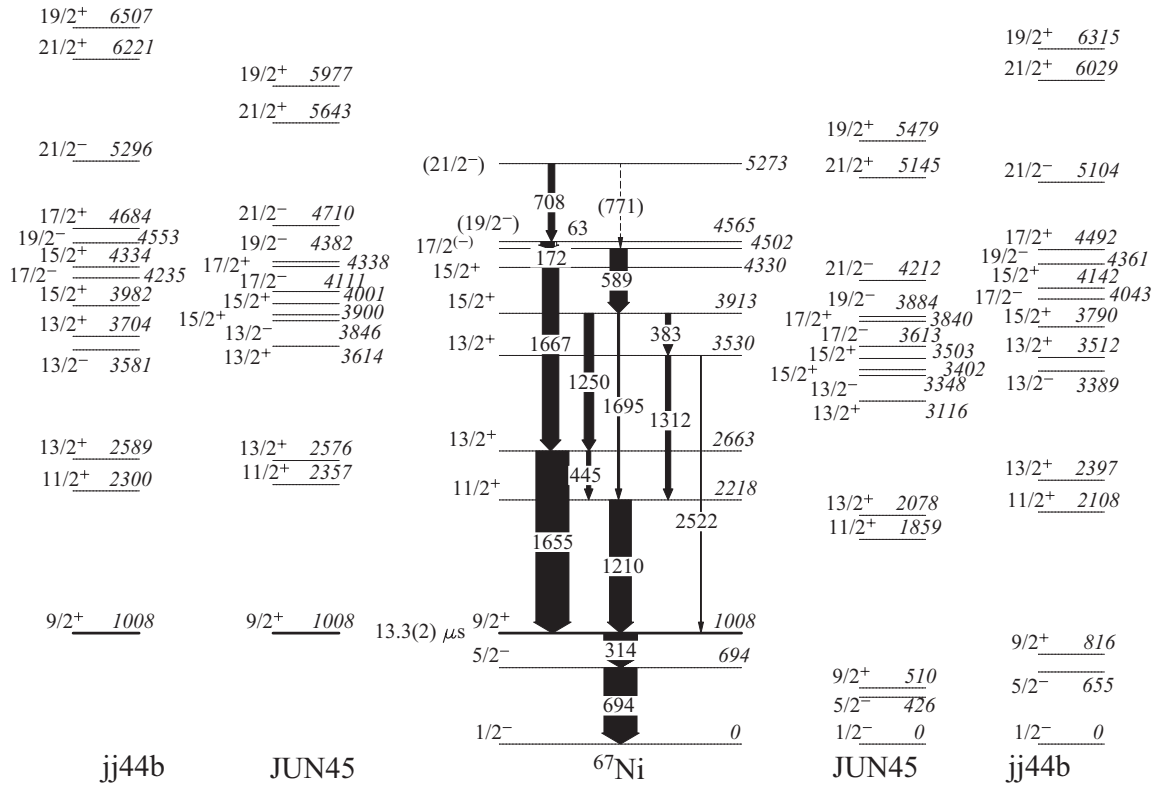
FIG. 5. Proposed level scheme of ^{67}Ni. Results of the shell-model calculations with the JUN45 and jj44b effective interactions are shown for comparison. The set of calculations to the left is identical to that on the right, except that the excitation energies were offset such that the $9/2^+$ isomeric state matches the data.

FIG. 6. Measured angular correlations for $\gamma\gamma$ cascades in ^{67}Ni. Dashed lines in the figure correspond to expected patterns associated with pairs of stretched quadrupole-quadrupole transitions [panels (a) and (b)], while the dot-dashed line is associated with a stretched quadrupole-dipole pair of γ rays (panel b).

comparison with the theoretical prediction of Fig. 6(a), which agrees with a $9/2^+ \rightarrow 5/2^- \rightarrow 1/2^-$ cascade. In view of the smaller intensities, the correlation between the 1655- and the 1667-keV lines was grouped into five angles [Fig. 6(b)]. It is consistent with a quadrupole-dipole sequence. To be consistent with the decay pattern of the 2663-keV level, the 1655-keV γ ray is proposed as a quadrupole transition, leading to a $13/2^+$ assignment for this state and $15/2^+$ quantum numbers for the level at 4330 keV.

Because of the lack of statistics, the correlation data for other transitions were regrouped into the two angles of $33°$ (from $20°$ to $42°$ in Gammasphere) and $77°$ ($69°$ to $87°$). Intensity ratios were obtained for the transition pairs of 1655-1250, 1655-172, and 1210-1695 keV. The ratio of 0.81(9) measured for the 1655-1250 keV cascade points to a dipole character for the 1250-keV γ ray, resulting in a $15/2^+$ assignment to the 3913-keV level. With this $15/2^+$ assignment and the measured 1.8(3) ratio indicating a quadrupole-dipole cascade for the 1210-1695 keV pair where the dipole transition has a large $E2/M1$ mixing ratio, a consistent picture emerges with the proposed $11/2^+$ spin and parity for the 2218-keV state. Note that the mixed-dipole character for the 1210-keV transition is also consistent with the expectations of shell-model calculations, as is discussed below. A $17/2$ spin assignment to the 4502-keV state was derived from the 0.85(4) correlation ratio measured for the 1655-172 keV pair. Even though correlation data could not be extracted for the 1210-1312 keV cascade, the $13/2^+$ assignment to the 3530-keV level is supported by the presence of the weak, 2522-keV decay branch toward the $9/2^+$ isomer. Finally, the general agreement between these assignments and the results of shell-model calculations was used to tentatively propose $19/2^-$ and $21/2^-$ assignments to the two highest states. The
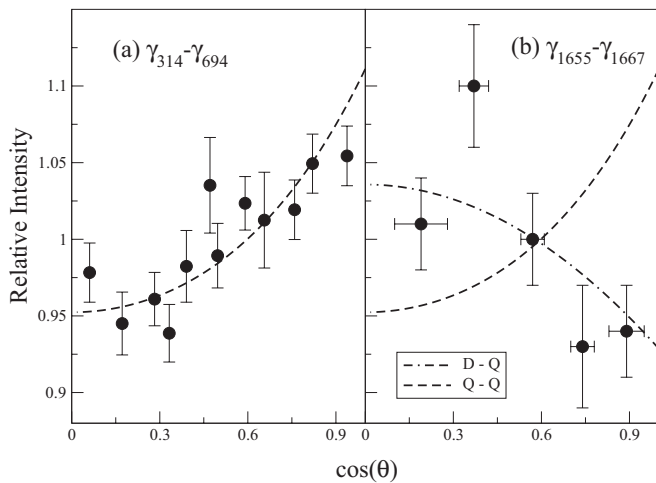
TABLE I. List of levels with the spin-parity assignments and γ rays identified in ^{67}Ni, including intensities and placements.

E_i (keV)	J_i^π	J_f^π	E_γ (keV)	I_γ
0	$1/2^-$			
694.3(2)[a]	$5/2^-$	$1/2^-$	694.3(2)	
1008.1(3)[a]	$9/2^+$	$5/2^-$	313.8(2)	
2218.0(4)	$11/2^+$	$9/2^+$	1210.0(3)	66(9)
2662.8(4)	$13/2^+$	$11/2^+$	444.9(3)	13(2)
		$9/2^+$	1654.7(2)	100(8)
3530.3(4)	$13/2^+$	$11/2^+$	1312.3(3)	16(3)
		$9/2^+$	2522(1)	2.0(5)
3913.0(4)	$15/2^+$	$13/2^+$	382.7(2)	16(3)
		$13/2^+$	1250.0(3)	29(5)
		$11/2^+$	1695.1(5)	7(1)
4330.1(4)	$15/2^+$	$13/2^+$	1667.3(2)	50(7)
4501.9(4)	$17/2^{(-)}$	$15/2^+$	171.8(2)	48(6)
		$15/2^+$	588.8(2)	52(6)
4564.7(5)	$(19/2^-)$	$17/2^{(-)}$	62.8(2)	31(6)
5273.1(7)	$(21/2^-)$	$(19/2^-)$	708.4(5)	20(3)
		$(21/2^-)$	$17/2^{(-)}$	771(1)	<3

[a]Observed only with beam off.

experimental information on levels in ^{67}Ni is summarized in Table I.

IV. DISCUSSION

At first glance, the level structure on top of the $9/2^+$ isomer in ^{67}Ni appears to be of single-particle character. The yrast sequence does not exhibit any regularity in the increase in excitation energy with angular momentum, as would be expected in the presence of collectivity, and states of opposite parity compete for yrast status. Moreover, in the absence of any notable Doppler shift for any of the observed transitions, the combined feeding and level lifetimes must be at least of the order of the stopping time of the reaction products in the thick uranium target, i.e., 1 ps or longer. It should also be noted that the sequence of levels above the $9/2^+$ isomer exhibits similarities with the structure found above the corresponding $9/2^+$ long-lived state in ^{65}Ni. The latter structure was interpreted in terms of single-particle excitations; see Ref. [29] for details. These observations would argue in favor of a subshell closure at $N = 40$.

In order to gain further insight into the nature of the observed ^{67}Ni states, large-scale calculations were carried out with the shell-model code ANTOINE [38,39] using both the jj44b [40] and the JUN45 [41] effective interactions. Both Hamiltonians were restricted to the $f_{5/2}$, $p_{3/2}$, $p_{1/2}$, and $g_{9/2}$ valence spaces and assume a ^{56}Ni core. However, the required two-body matrix elements and single-particle energies were obtained from fits to different sets of data. Specifically, the JUN45 interaction was developed by considering data in nuclei with $Z \sim 32$ and $N \sim 50$ and excludes explicitly the Ni and Cu isotopes as the ^{56}Ni core is viewed as being rather "soft" [41]. In contrast, experimental data from $Z = 28$–30 isotopes and

$N = 48$–50 isotones were incorporated in the fits in the case of the jj44b interaction [40].

The results of the calculations are compared with the experimental data in Fig. 5. With both interactions, the energy of the $9/2^+$ state is predicted lower than the measured value. This can be viewed as an indication that the adopted single-particle energy of the $g_{9/2}$ neutron orbital is too low in the two Hamiltonians. It is worth noting that the jj44b interaction calculates this state to lie within 192 keV of the data and indicates about a 25% admixture of the $\nu g_{9/2}^3$ configuration into the $9/2^+$ wave function. With the JUN45 interaction, the level is predicted to lie 498 keV lower than in the data with roughly 33% of the wave function involving three neutrons in the $g_{9/2}$ orbital. This is possibly the result of the location of the $g_{9/2}$ orbital at a lower energy in the JUN45 Hamiltonian, as compared to that used in the jj44b case, which leads to larger configuration mixing in the wave function of the $9/2^+$ state.

Overall, the calculated spectrum with both interactions appears somewhat compressed when compared to the data, as illustrated on the right side of Fig. 5. Note that for reasons of clarity, only the calculated yrast and near-yrast excitations are shown; i.e., the states with a likely corresponding level in the data are plotted. The correspondence between data and calculations is rather satisfactory when the computed excitation energies are expressed relative to the $9/2^+$ isomer as is done on the left-hand side of Fig. 5. Indeed, both interactions predict close-lying $11/2^+$ and $13/2^+$ levels, separated from the next $13/2^+$ excitation by roughly 1 MeV, in agreement with the proposed level scheme. A pair of close-lying $15/2^+$ levels is also computed to be located directly above the $13/2_2^+$ state, as seen in the data. Both interactions also predict a first excited $17/2^+$ state more than 300 keV above the $15/2_2^+$ excitation with higher-spin, positive-parity states another 1.3 MeV or more above this. In contrast, negative-parity levels are present at lower excitation energies with both effective interactions, leading to the proposed assignments of $17/2^{(-)}$, $(19/2^-)$, and $(21/2^-)$ for the 4502-, 4565-, and 5273-keV states in Fig. 5. As indicated in the figure, these assignments should be viewed as tentative, especially in the case of the $17/2$ level, where calculated $17/2$ states of both parities are separated only by $\sim$200 and $\sim$400 keV, depending on the interaction.

It is of interest to identify in the calculations the main components of the wave functions of the observed states. For the $11/2^+$ level, and the nonyrast $13/2_2^+$ and $15/2_2^+$ states, both Hamiltonians result in wave functions in which the $\nu f_{5/2}^5 p_{3/2}^4 p_{1/2}^1 g_{9/2}^1$ configurations dominate with a contribution of the order of 50%. Perhaps surprisingly, the $13/2_1^+$ and $15/2_1^+$ states are computed to be more fragmented, with respective main contributions by the $\nu f_{5/2}^5 p_{3/2}^4 p_{1/2}^1 g_{9/2}^1$ and $\nu f_{5/2}^4 p_{3/2}^4 p_{1/2}^2 g_{9/2}^1$ configurations of $\sim$30% only. In addition, the JUN45 interaction results in a $\sim$10% admixture of the $\nu g_{9/2}^3$ configuration into the wave functions of these two levels. This contribution is of the order of 5% with the jj44b interaction. With this Hamiltonian the wave functions of all the negative-parity states are mixed with only the $17/2^-$ level having a contribution from the $\nu f_{5/2}^4 p_{3/2}^4 p_{1/2}^1 g_{9/2}^1$ of the order of 50%. In contrast, with the JUN45 interaction, where the

TABLE II. Relative branching ratios depopulating the $13/2_1^+$, $13/2_2^+$, and $15/2_1^+$ levels derived from experimental measurements, and calculated results using the JUN45 and jj44b effective interactions.

J_i^π	J_f^π	Measurements	JUN45[a]	jj44b[a]	JUN45[b]	jj44b[b]
$13/2_1^+$	$11/2^+$	13(2)	6	23	36	67
	$9/2^+$	100(8)	100	100	100	100
$13/2_2^+$	$13/2_1^+$	<3	0	166	0	96
	$11/2^+$	100(20)	100	100	100	100
	$9/2^+$	11(4)	9	105	7	92
$15/2_1^+$	$13/2_2^+$	57(9)	33	11	95	40
	$13/2_1^+$	100(15)	100	100	100	100
	$11/2^+$	23(2)	15	5	28	7

[a]Branching ratios are obtained with calculated transition energies.
[b]Branching ratios are obtained with measured transition energies.

ordering of states is computed in better agreement with the data [see the $15/2_2^+$–$17/2^{(-)}$–$(19/2^-)$–$(21/2^-)$ sequence in Fig. 5], the wave function of every negative-parity state is characterized by a 40–50% component from the $\nu f_{5/2}^4 p_{3/2}^4 p_{1/2}^1 g_{9/2}^2$ configuration.

In the absence of lifetime information on the ^{67}Ni levels above the isomer, additional tests of the shell-model calculations are possible by considering the branching ratios for transitions competing in the de-excitation of specific levels. For the computation of the $B(E2)$ transition probabilities, proton and neutron effective charges $e_p = 1.5e$ and $e_n = 0.5e$ were adopted as is usual for nuclei in this region. Comparisons between computed branchings for the two Hamiltonians and the data are presented in Table II. Only cases for which the coincidence yields were sufficient to allow gating on the transitions directly feeding a state of interest were considered for Table II. Note that this table provides shell-model results using either the calculated or the measured transition energies. The latter values effectively remove the dependence of the ratios on the transition energies. From the table, it is clear that calculations with the JUN45 Hamiltonian are consistently in better agreement with the measured branching ratios. It is also worth pointing out that both Hamiltonians also compute a $11/2^+ \rightarrow 9/2^+$ transition of strongly mixed $E2/M1$ character ($|\delta| > 0.5$), in agreement with the angular-correlation data for the 1210- to 1695-keV cascade (see Sec. III).

From the discussion above, it is concluded that the levels above the $9/2^+$ isomeric state can be understood as neutron excitations, with contributions of protons across the $Z = 28$ gap playing a minor role at best. Calculations with both interactions are in fair agreement with the data. They attribute a significant role to the $g_{9/2}$ neutron orbital for every state observed in this measurement. In fact, in most cases, significant $\nu g_{9/2}^2$ and $\nu g_{9/2}^3$ configurations are part of the wave functions. Similar observations have been made for other nuclei close to ^{68}Ni; see, for example, recent comparisons between calculations with the same jj44b and JUN45 interactions and data for ^{65,67}Cu in Ref. [42]. From these findings, it is concluded that even in a nucleus only one neutron removed from $N = 40$, the impact of a neutron shell closure is rather modest. As the $g_{9/2}$ neutron orbital is shape driving, multi-particle-hole excitations

involving this state may be expected to be associated with enhanced collectivity and it would be of interest to investigate the latter in future measurements.

V. CONCLUSIONS

A level scheme above the known 13-μs isomer in ^{67}Ni was established by exploring prompt and delayed coincidence relationships from deep-inelastic reaction products. Spin and parity quantum numbers for the newly observed states were deduced from an angular-correlation analysis whenever sufficient statistics were available. Shell-model calculations have been carried out with two modern effective interactions, JUN45 and jj44b, for the $f_{5/2}pg_{9/2}$ model space with ^{56}Ni as a core. Satisfactory agreement between experiment and theory was achieved. Even though the level structure of ^{67}Ni appears to exhibit a single-particle character based on comparisons between the measured level properties, including branching ratios, with the results of shell-model calculations, it is suggested that the yrast and near-yrast states are associated with rather complex configurations. In fact, calculations indicate that the wave functions of the yrast states involve a large number of configurations without a dominant ($\sim$50%) specific one, the latter being more prevalent in the near-yrast levels. It is hoped that the present data will stimulate additional theoretical work such as comparisons with calculations using other effective interactions or a different model space. Further experimental work aimed at the evolution of the degree of collectivity with spin and excitation energy is highly desirable as well.

[1] O. Sorlin and M.-G. Porquet, Prog. Part. Nucl. Phys. **61**, 602 (2008).

[2] R. V. F. Janssens, Nature (London) **459**, 1069 (2009).

[3] M. Bernas, Ph. Dessagne, M. Langevin, J. Payet, F. Pougheon, and P. Roussel, Phys. Lett. B **113**, 279 (1982).

[4] R. Broda et al., Phys. Rev. Lett. **74**, 868 (1995).

[5] R. Grzywacz et al., Phys. Rev. Lett. **81**, 766 (1998).

[6] T. Ishii, M. Asai, A. Makishima, I. Hossain, M. Ogawa, J. Hasegawa, M. Matsuda, and S. Ichikawa, Phys. Rev. Lett. **84**, 39 (2000).

[7] O. Sorlin et al., Phys. Rev. Lett. **88**, 092501 (2002).

[8] N. Bree et al., Phys. Rev. C **78**, 047301 (2008).

[9] C. Guénaut et al., Phys. Rev. C **75**, 044303 (2007).

[10] S. Rahaman et al., Eur. Phys. J. A **34**, 5 (2007).

[11] K. Langanke, J. Terasaki, F. Nowacki, D. J. Dean, and W. Nazarewicz, Phys. Rev. C **67**, 044314 (2003).

[12] M. Hannawald et al., Phys. Rev. Lett. **82**, 1391 (1999).

[13] W. F. Mueller et al., Phys. Rev. Lett. **83**, 3613 (1999).

[14] O. Sorlin et al., Eur. Phys. J. A **16**, 55 (2003).

[15] L. Gaudefroy et al., Eur. Phys. J. A **23**, 41 (2005).

[16] P. Adrich et al., Phys. Rev. C **77**, 054306 (2008).

[17] A. Gade et al., Phys. Rev. C **81**, 051304 (2010).

[18] J. Ljungvall et al., Phys. Rev. C **81**, 061301(R) (2010).

[19] W. Rother et al., Phys. Rev. Lett. **106**, 022502 (2011).

[20] O. Perru et al., Phys. Rev. Lett. **96**, 232501 (2006).

[21] T. Otsuka, R. Fujimoto, Y. Utsuno, B. A. Brown, M. Honma, and T. Mizusaki, Phys. Rev. Lett. **87**, 082502 (2001).

[22] T. Otsuka, T. Suzuki, R. Fujimoto, H. Grawe, and Y. Akaishi, Phys. Rev. Lett. **95**, 232502 (2005).

[23] A. N. Deacon et al., Phys. Lett. B **622**, 151 (2005).

[24] S. Zhu et al., Phys. Rev. C **74**, 064315 (2006).

[25] A. N. Deacon et al., Phys. Rev. C **83**, 064305 (2011).

[26] A. N. Deacon et al., Phys. Rev. C **76**, 054303 (2007).

[27] N. Hoteling et al., Phys. Rev. C **77**, 044314 (2008).

[28] I. Stefanescu et al., Phys. Rev. C **79**, 034319 (2009).

[29] T. Pawłat et al., Nucl. Phys. **A574**, 623 (1994).

[30] L. Weissman et al., Phys. Rev. C **59**, 2004 (1999).

[31] J. Rikovska et al., Phys. Rev. Lett. **85**, 1392 (2000).

[32] G. Georgiev et al., J. Phys. G **28**, 2993 (2002).

[33] R. V. F. Janssens et al., Phys. Lett. B **546**, 55 (2002).

[34] B. Fornal et al., Phys. Rev. C **72**, 044315 (2005).

[35] R. Broda, J. Phys. G **32**, R151 (2006).

[36] I.-Y. Lee, Nucl. Phys. A **520**, 641c (1990).

[37] N. Hoteling et al., Phys. Rev. C **74**, 064313 (2006).

[38] E. Caurier and F. Nowacki, Acta Phys. Pol. B **30**, 705 (1999).

[39] E. Caurier, shell-model code ANTOINE (IRES, Strasbourg, 1989–2004).

[40] B. A. Brown (private communication); see also Ref. [28] in B. Cheal et al., Phys. Rev. Lett. **104**, 252502 (2010).

[41] M. Honma, T. Otsuka, T. Mizusaki, and M. Hjorth-Jensen, Phys. Rev. C **80**, 064323 (2009).

[42] C. J. Chiara et al., Phys. Rev. C **85**, 024309 (2012).